

Quantifying multi-point ordering in alloys

James M. Goff,^{1,*} Bryant Y. Li,¹ Susan B. Sinnott,^{1,2,3} and Ismaila Dabo^{1,3,4}

¹*Department of Materials Science and Engineering,*

The Pennsylvania State University, University Park, PA 16802, USA

²*Department of Chemistry, The Pennsylvania State University University Park PA 16802, USA*

³*Materials Research Institute, The Pennsylvania State University, University Park, PA 16802, USA*

⁴*Penn State Institutes of Energy and the Environment,*

The Pennsylvania State University University Park PA 16802, USA

A central problem in multicomponent lattice systems is to systematically quantify multi-point ordering. Ordering in such systems is often described in terms of pair correlations, even though this is not sufficient when three-point and higher-order interactions are significant. Current models and parameters for multi-point ordering are often only applicable for very specific cases and/or require approximating a subset of correlated occupational variables on a lattice as being uncorrelated. In this work, a multi-point cluster order parameter is introduced to quantify arbitrary multi-point ordering motifs in substitutional systems through direct calculations of normalized cluster probabilities. These parameters can describe multi-point chemical ordering in crystal systems with multiple sublattices, multiple components, and systems with reduced symmetry. These are defined within and applied to quantify four-point chemical ordering motifs in platinum/palladium alloy nanoparticles that are practical interest to the synthesis of catalytic nanocages. Impacts of chemical ordering on alloy nanocage stability are discussed. It is demonstrated that approximating multi-point order parameters from combinations of low-order correlations is not sufficient in cases where multi-point energetics are significant. Conclusions about the formation mechanisms of nanocages may change significantly when using common low-order approximations.

* jmg670@psu.edu

I. INTRODUCTION

Chemical ordering in alloys and other multicomponent crystal systems strongly influences material properties such as mechanical strength, durability, and thermodynamic stability. This includes both the long-range periodic arrangement of elements in ordered alloys such as Cu_3Au and the short-range order (SRO) that occurs in solid solution crystal systems over shorter distances.[1] In alloys, SRO can influence the thermodynamic stability as well as mechanical properties; increased SRO in CrCoNi alloys leads to increased hardness.[2, 3] In semiconductors, the optical and electronic properties are influenced by the chemical ordering.[4] At the solid-solution interfaces of alloy catalysts, the adsorption of solution species is correlated with alloy ordering and this influences the electrochemical response.[5] In the case of platinum-based alloy nanoshells applied in hydrogen fuel cells as oxygen reduction catalysts, the chemical SRO and structure of the surface alloy have a strong influence on catalyst durability.[6] In these catalytic surface alloys and many other cases, such as in high-entropy oxides, semiconductor crystals with multiple sublattices, and other catalyst systems, the chemical ordering motifs of interest are comprised of multiple points and may span multiple sublattices.[5, 7, 8] Due to the strong interdependence between SRO and material properties, it is desirable to systematically quantify chemical ordering in substitutional systems.

The Warren-Cowley SRO parameters are among the most commonly used descriptors for pair ordering in alloys, both experimentally and theoretically.[9–14] These parameters can be written for binary systems as

$$\gamma_m^{pq} = 1 - \frac{P(q|p)_m}{c_q}. \quad (1)$$

The parameter is given in terms of the conditional probability that atom p is at a site with atom q in some neighbor shell around it, labeled by m (Fig. 1A). These probabilities, which can be obtained by inversion of pair correlations, are then divided by the concentration c_q . In a random alloy the pair parameter is 0, when $\gamma_m^{pq} > 0$ there is a tendency of p - q ordering, and when $\gamma_m^{pq} < 0$ there is a tendency of p - p and q - q pair ordering. While the description of chemical SRO in terms of pair ordering is useful in many cases; pairs alone do not completely describe a substitutional system. For example in Fig. 1B, the Warren-Cowley parameters do not describe the ordering motif where a blue atom occupies a site adjacent to a grey-blue pair, a three-point correlation. It also cannot describe a three-point correlation between sublattices in an alloy oxide. While correlations with 3+ bodies of this sort are often less significant than pair correlations, all of the n -body correlations (and n -body orderings) are needed to completely describe a system.[15] Many alloys and substitutional crystal systems can be represented with an Ising-like Hamiltonian that depends on chemical occupation variables of sites in the lattice. In such models, it has been proven that correlations up to the order of the interactions in the Hamiltonian are required to completely describe the system.[16] Neglecting high-order correlations can lead to poor predictions of material properties, as in the inverse Monte Carlo method.[17–19] Incorporation of high-order correlations and associated SRO into models and analysis of substitutional systems would be beneficial, but it is often dismissed due to challenges in obtaining of the multi-point probabilities both experimentally and theoretically.

A number of other developments have been made to extend the Warren-Cowley parameters beyond their typical application to pair-ordering in AB alloys, including the extension of the Warren-Cowley parameters to systems with more than two components.[20, 21] Work by Clapp showed that some multi-point correlations, and therefore the multi-point probabilities needed for general order parameters, can be obtained from lower order ones through the Kirkwood superposition (multiplication of pair probabilities).[22–25] In special cases such as linear binary chains or in equimolar A-B alloys, some of the high-order correlations may be exactly expressed in terms of lower order pair and single-site correlations. In general this is approximate and not suitable for systems with highly correlated lattice occupations or with strong multi-point interactions.[16, 23] Similar approximations have been made by Shirley and Wilkins, reconstructing multi-point correlations from pair combinations contained in the motif.[26, 27] This method still approximates the occupations of correlated lattice sites contained in the motif as combinations of pairs that occur independently from one another. Its main utility is at the order/disorder transition temperature. Definitions of multi-point order parameters were included in Shirley and Wilkins, but these suffer from the deficiencies associated with the approximated multi-point correlations used to define them. It was proven in Nicholson et al. and demonstrated in other works, that such methods only work in cases where interactions beyond pairs are negligible.[28] Obtaining multi-point orderings from pair correlations can be highly successful when pairs or effective pair interactions are sufficient, as demonstrated by various computational and theoretical models.[29, 30] Some three-point and four-point ordering parameters have been defined and used for stochastic generation of 2D substitutional lattices possessing high-order correlations.[31, 32] Methods such as the geometrical locus method that quantify the ordering of derivative structures are currently limited to specific crystal systems and motifs.[33–35] Exact quantification of general multi-point orderings is still needed for substitutional with multiple components and between sublattices. Approximating these from low order correlations is desirable for connection to experimental SRO intensities, but as we show within,

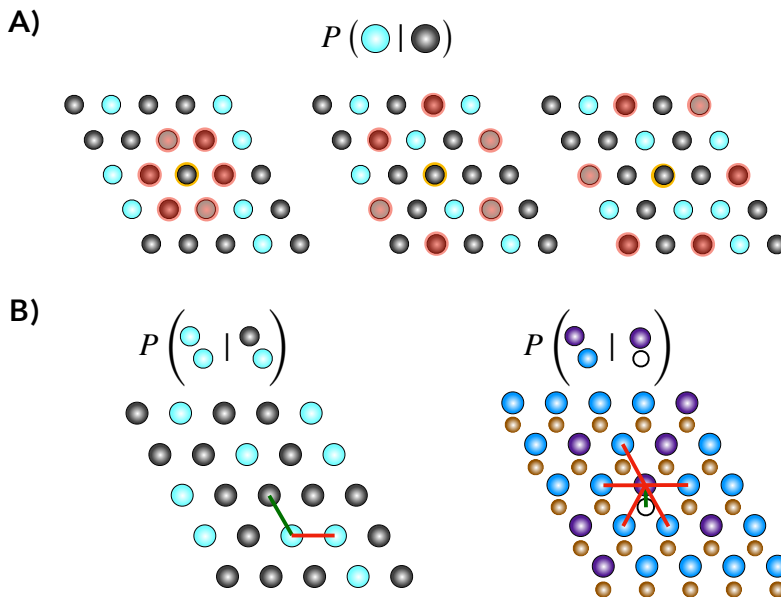


Figure 1: A) Pair ordering in alloys is described in terms of the conditional probability of finding a B atom in a nearest neighbor shell around an A atom in an AB alloy and is often quantified with the Warren Cowley pair order parameters. A single pair parameter alone cannot describe multi-point ordering motifs in B).

does not apply well for systems with important many-point interactions.

The extraction of three-point and higher correlations from crystals in x-ray experiments is still an active area of study.[36–39] Impressive strides have been made in energy-resolved scanning tunneling electron microscopy to directly measure SRO domains in alloys, but atomic-level chemical ordering across multiple points in alloy systems is still challenging to quantify.[3, 40] Simulation and theory could be used to directly evaluate multi-point chemical ordering to support experimental findings, but it can be challenging to obtain meaningful statistics in substitutional/alloy systems with many degrees of freedom. The notions of statistical efficiency and accuracy need to be addressed as descriptors of chemical ordering, such as the Warren-Cowley parameter, are extended to multi-point motifs. This was partly addressed by the work of de Fontaine when the order parameters were recast as normalized pair probabilities, and the number of independent pair parameters were defined for systems with arbitrary numbers of components. We aim to extend the description of normalized probabilities to multi-point ordering in alloys. In this work, a set of cluster order parameters are introduced for systematically quantifying multi-point ordering in multicomponent crystals through direct measurements of normalized cluster probabilities.

II. DEFINING THE CLUSTER ORDER PARAMETERS

A. Order parameters on a single sublattice

We define a set of order parameters to quantify arbitrary multi-point chemical ordering. Like the Warren-Cowley parameters and the current three- and four-point parameters in the literature, the new set of parameters should be 0 for the disordered phase. To begin, an occupation variable representation of a single substitutional lattice is adopted, much like that for Ising or cluster expansion models. The occupations of sites on a lattice are designated by a collection of variables as a occupation/spin vector,

$$\vec{\sigma} = \{\sigma_1, \sigma_2, \sigma_3 \dots \sigma_N\} \quad (2)$$

A spin variable σ_i is assigned to each lattice site of an N -site crystal. The spin variables are integers that take on the values:

$$\sigma_i = \begin{cases} -m, -m+1, \dots -1, 1, \dots m+1, m : & m = d/2 \\ -m, -m+1, \dots -1, 0, 1, \dots m+1, m : & m = (d-1)/2 \end{cases} \quad (3)$$

where the first case occurs when the compositional degrees of freedom for a lattice site, d , are even and the second case when the degrees of freedom are odd. In a binary alloy containing two species A and B, the spin variables can take the values $\sigma_i = \{-1, 1\}$ corresponding to A and B, respectively.

We are interested in developing an order parameter for arbitrary collections of lattice points in a crystal. The complete, orthonormal set of basis functions defined for the discrete variable space in Eq. (2) are a convenient starting point.[15] All distinct collections of lattice points are contained in this set of cluster basis functions. This set of basis functions, is presented as:

$$\{\Phi_\alpha(\vec{\sigma}_\alpha)\}, \quad (4)$$

where the basis function, Φ_α , for a cluster, α and depends on the spin variables of the sites contained in the cluster, $\vec{\sigma}_\alpha$. The set of basis functions includes an empty identity cluster for completeness, single-site, pairs, triplets, quadruplets, and so on. The expectation values of these are the correlation functions and can be written as:

$$\bar{\Phi}_\alpha(\vec{\sigma}) = \frac{1}{m_\alpha N} \sum_{\beta=\alpha}^{N_p} \sum_p \Phi_\beta(\vec{\sigma}_\beta(p)), \quad (5)$$

where the inner sum runs over all distinct locations of the a cluster, p , and the outer sum runs over all symmetrically equivalent clusters, $\beta = \alpha$. Per-site correlations are obtained by dividing by the number of lattice sites, N , and the number of symmetrically equivalent clusters, m_α . It is noted that the number of distinct cluster locations, N_p , may differ from the total number of sites, N , in crystals with reduced symmetry, such as a 2D surface with a set thickness. This is the case in the example given later.

The correlations in Eq. (5) can be written in terms of occupational pair, triplet, quadruplet etc. probabilities as a weighted average.

$$\bar{\Phi}_\alpha(\vec{\sigma}) = \frac{N_p}{N} \sum_{\vec{\sigma}_\alpha} \Phi_\alpha(\vec{\sigma}_\alpha) \bar{P}(\vec{\sigma}_\alpha) \quad (6)$$

Here, the sum now runs over all distinct occupations of the cluster multiplied by the respective probability of finding any symmetrically equivalent cluster with that specific occupation in the crystal, $\bar{P}(\vec{\sigma}_\alpha)$. These probabilities, referred to as cluster probabilities, can be defined as:

$$\bar{P}(\vec{\sigma}_\alpha) = \frac{1}{m_\alpha N_p} \sum_{\beta=\alpha} n(\vec{\sigma}_\beta). \quad (7)$$

The total number of clusters with the desired occupation is counted at each distinct location, p , in the crystal to give $n(\vec{\sigma}_\alpha)$. The counts are summed over all symmetrically equivalent clusters, and divided by the symmetry multiplicity and total number of occurrences of the cluster in the crystal, N_p . These probabilities sum to 1:

$$\sum_{\vec{\sigma}_\alpha} \bar{P}(\vec{\sigma}_\alpha) = 1. \quad (8)$$

The sum is taken over all possible distinct occupations of the cluster.

Using the multi-point probabilities defined in Eq. (7), the general cluster order parameter is introduced.

$$\gamma_\alpha = 1 - \frac{\bar{P}(\vec{\sigma}_\alpha^d)}{P_{\text{random}}} \quad (9)$$

where the order parameter, γ_α is given in terms of the average probability of finding a cluster with a desired occupation, $(\vec{\sigma}_\alpha^d)$ in the crystal that is normalized by the probability of the cluster forming with the desired occupation in a random alloy, P_{random} . In the random alloy the probability of a site being occupied by a specific species, $P(\sigma_i)$, is given by the atomic concentration of that species C_i ; the probability in the denominator is the product of the site probabilities for a given cluster occupation. For example, P_{random} in an AB alloy for a three-point occupation of $(\vec{\sigma}_\alpha^d) = [-1, -1, -1]$ corresponding to (AAA) is given by $C_A C_A C_A$. It can be directly shown that by selecting a pair cluster, $\alpha \in \{\text{pairs}\}$ the cluster order parameter reduces to the binary Warren-Cowley SRO parameters.

The analysis of the cluster order parameters is similar to that for the Warren-Cowley pair parameters.[10] When the cluster order parameter, $\gamma_\alpha = 0$ then the cluster shape with the specified occupation occurs as frequently as it

would in a random alloy. When $\gamma_\alpha > 0$ then the cluster with the specified occupation is found less often than in a random alloy of the same composition. Finally, when $\gamma_\alpha < 0$ then the cluster with desired occupation occurs more frequently than in a random alloy. Limiting values of the cluster order parameters may be related to long-range or superstructure orderings depending on the cluster and crystal. The limits of the cluster order parameters at large separations could be used to generalize long-range order parameters.[41]

Special cases of derivative structure orderings and multi-point motifs can be inferred by the geometrical locus method. Recall that the generalized geometrical locus method provided constraints on the pair parameters spanning derivative polyhedra in certain AB crystals (rocksalt, CsCl structure, and SnS structure).[33, 34] The ordering of octahedra in the rocksalt lattice can be inferred based on composition, whether or not the octahedra are arranged periodically, the composition of the octahedron, and noting that the octahedra span the crystal. With the cluster order parameter formalism, the ordering of octahedra (or other derivative polyhedra) can be directly measured with polyhedral 'cluster'. Defining similar with the cluster probabilities could allow for a generalization of the geometrical locus method to derivative structures beyond polyhedra, and alloys with more than two components.[42]

B. Order parameters on multiple sublattices

The cluster order parameter can be generalized to crystals with multiple sublattices. This is demonstrated in a two sublattice system for example. The occupations of the sites in each respective are designated with a spin vector, $\vec{\sigma}$ and $\vec{\delta}$ as in Eq. (2) of the main text. A set of cluster basis functions can be assigned to each sublattice, $\{\Phi_\alpha^1(\vec{\sigma})\}$ and $\{\Phi_\alpha^2(\vec{\delta})\}$. A complete set of composite basis functions can be defined for the multi-lattice crystal by taking the tensor product of the single sublattice clusters spaces.[43] Using a similar notation as in Tepesch et al. in 1995 these composite basis functions, indexed by θ , are denoted as:

$$\{\Theta_\theta(\vec{\tau}_\theta)\} \quad (10)$$

where we have defined a single vector containing the spin variables for the entire crystal.

$$\vec{\tau} = (\sigma_1, \sigma_2, \dots, \sigma_{N_1}, \delta_1, \delta_2, \dots, \delta_{N_2}) \quad (11)$$

The inter and single-sublattice correlations are given as the expectation value of the composite basis functions over the crystal. These are calculated as

$$\bar{\Theta}_\theta(\vec{\tau}) = \frac{1}{m_\theta N} \sum_{\phi=\theta} \sum_c^{N_c} \Theta_\phi(\vec{\tau}_\phi(c)). \quad (12)$$

The inner sum runs over all distinct locations of the composite cluster, c , and the outer sum now runs over all symmetrically equivalent composite clusters, $\theta = \phi$. The sum of the evaluated composite cluster functions at all of these points is then divided by the total number of sites in the crystal coming from sublattices 1 and 2, $N = (N_1 + N_2)$, multiplied by the number of symmetrically equivalent composite clusters, m_θ .

The correlations in Eq. (12), can also be written as weighted averages of cluster basis functions evaluated for specific *cluster* occupations following a similar form as that for a single sublattice.

$$\bar{\Theta}_\theta(\vec{\tau}) = \frac{N_c}{N} \sum_{\vec{\tau}_\theta} \Theta_\theta(\vec{\tau}_\theta) \bar{P}(\vec{\tau}_\theta) \quad (13)$$

where the sum now runs over all occupations possible in the composite cluster. The multi-point probabilities for the inter-sublattice correlations are defined as

$$\bar{P}(\vec{\tau}_\theta) = \frac{1}{m_\theta N_c} \sum_{\phi=\theta} n(\vec{\tau}_\phi). \quad (14)$$

The counts of composite clusters with a specific inter-sublattice occupation, τ_θ , are summed for all symmetrically equivalent composite clusters and divided by the total number of occurrences of the composite cluster in the crystal, N_c , multiplied by the symmetry multiplicity. With this, the inter-sublattice cluster order parameter can be defined.

$$\gamma_\theta = 1 - \frac{\bar{P}(\vec{\tau}_\theta^d)}{P_{\text{random}}} \quad (15)$$

The correlations in Eq. (13) could also be inverted to obtain specific probabilities. In the case of the composite cluster formed by the product of the two single-site basis functions, $\Theta([\sigma_i, \delta_j]) = \Phi_{\text{single}}^1(\sigma_i)\Phi_{\text{single}}^2(\delta_j)$, the inter-sublattice pair probabilities could be extracted. Because correlations beyond pairs can be considered, the ordering of cations about an anion vacancy could be considered in the rocksalt crystal structure for example.[8] Pair ordering alone would likely show a large tendency of unlike pair ordering between the cation and anion species.[44]

III. APPLICATION TO PT-BASED ALLOY NANOSHELL CATALYST

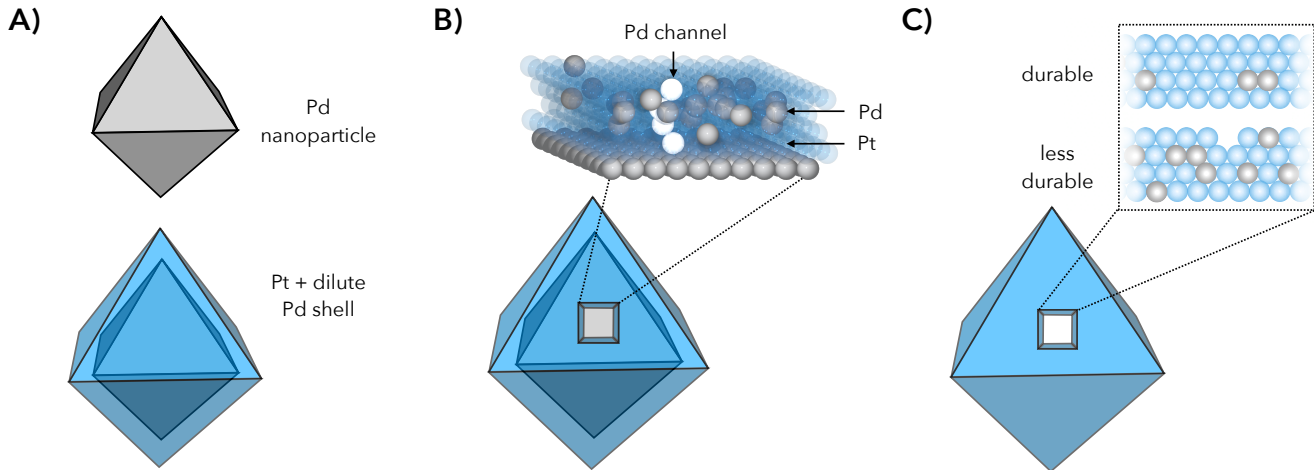


Figure 2: The palladium (111) fcc nanoparticles coated with a few atomic layers of a Pt/Pd alloy, A), prepared in Zhang 2015 rely on specific multi-point chemical ordering motifs, palladium channels that span the surface alloy region B), to generate high-surface area catalyst cages for the oxygen reduction reaction, C). A sufficient amount of Pd is needed to observe the 'channel' order motif in B) to allow for the etching of the palladium core but not so much that it diminishes the catalyst durability.

The need for an exact description of chemical SRO is highlighted in the case of platinum-based nanoshells in Fig. 2.[6] To make the platinum-based nanoshells, thin layers of dilute Pt/Pd alloy are deposited on palladium nanoparticles. The Pd cores are subsequently leached out leaving a highly active, predominantly Pt shell (10% Pd). Though the thicknesses of these catalyst shells are as low as 4 atomic layers, this resembles the surface of many other core-shell and alloy interfaces.[45–47] As evidenced in Zhang et al., the formation of Pd channels that span, or nearly span the deposited surface alloy, allow for subsequent etching of the Pd cores. They also found that excess Pd content decreased mechanical stability of the shells. Nanoshell catalysts with increased durability could potentially be produced by decreasing the Pd content while still allowing for Pd channel formation, Fig. 2B.

Pair ordering analysis would provide some insights into the Pd channel content in alloy surfaces, but the pair approximations used to quantify the Pd channel occurrence is somewhat arbitrary. The cluster order parameter was used instead to directly quantify Pd channel content in models of this alloy surface, and was compared to an approximated channel parameter constructed from pair probabilities. The surface of these alloy-coated nanoparticles were modeled using cluster expansions fit with and without a continuum solvent interface above the alloy surface to simulate some effects of the experimental environment.[48, 49] In these models, the (111) fcc surface was represented with 4 layers of Pt/Pd alloy on top of four pure palladium layers to represent the palladium core. The occurrence of four-point Pd channels spanning the alloy region determines whether the catalyst can be synthesized and its durability.

A. Model for the alloy surface

1. Density functional theory calculations

A selection of 398 symmetrically unique alloy configurations were used as training data for the cluster expansion. Some examples are provided in Fig. 3. The mixing energies of these alloy configurations were calculated using density functional theory. The surface alloy slabs were comprised of 8 layers in total with a vacuum height of 6 Å on either

side. Four of the layers on the bottom were pure Pd to represent the Pd core of the nanoparticles where the top four layers were comprised of both Pt and Pd with varied concentration. The DFT calculations were performed using the Quantum Espresso suite with plane wave basis sets.[50] The kinetic energy cutoff for the basis sets was 100 Ry. Norm conserving pseudopotentials from the PSEUDOJOJO library were used to represent ion cores.[51] An approximately uniform distribution of reciprocal Bloch vectors (\mathbf{k} -points) was used to sample the Brillouin zone across the cells by using the \mathbf{k} -point density of $(11/m \times 11/n \times 1)$ for an $m \times n$ surface cell. Electronic occupations were smoothed with 0.001 Ry of Marzari-Vanderbilt smearing.[52] The \mathbf{k} -points, smearing, slab thickness, energy cutoffs, and vacuum height were converged with respect to the Fermi energy of the system, to within 0.05 eV, ensuring that the interfacial dipole was converged. During geometry optimizations of surface alloy slabs the bottom two layers of Pd were fixed at calculated bulk lattice parameters, and total forces were below 25 meV/Å.

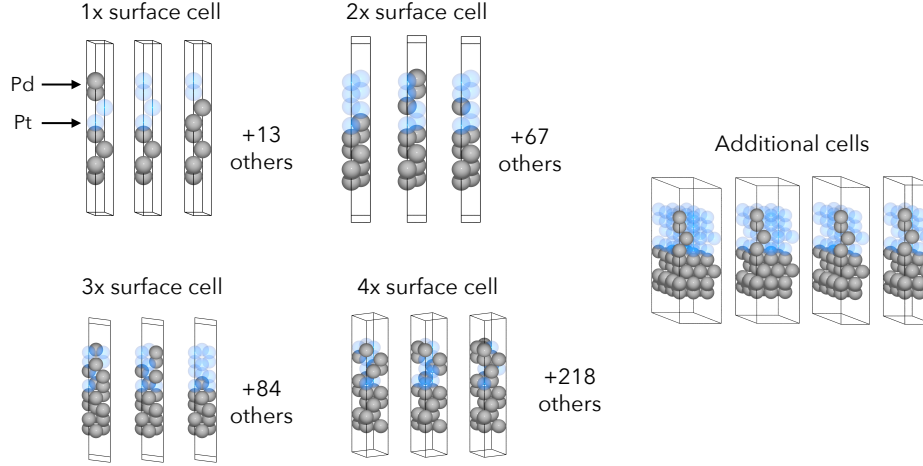


Figure 3: Examples of DFT surface cells used to fit the cluster expansion coefficients (grouped as multiples of the primitive surface cell). All symmetrically distinct configurations in the 1X and 2X cells are used for fitting along with larger randomized surface cells.

To account for average solvent effects on the surface alloy, the DFT energies for the surface alloy configurations were also calculated in the presence of a continuum solvent via the Self-Consistent Continuum Solvation method.[49] The shape and onset of the dielectric cavity are defined using minimum and maximum charge density cutoffs ($\rho_{\min} = 0.0013$ and $\rho_{\max} = 0.01025$) the original switching function provided in Andreussi, Dabo, and Marzari was used. The dielectric constant inside the cavity is 1 and switches smoothly to a dielectric constant of 78.3 outside the cavity. Surface tension, pressure, and volume terms were omitted as in Huang et al.[53] Though the DFT fitting cells in Fig. 3 are not symmetric, the contributions from solvent on the palladium core side should cancel out when calculating the mixing energies. Models including explicit solvation, adsorption of solution ions, and the etchant will likely show a stronger influence on the surface alloy structure and would help determine solvent conditions suitable for making more durable cages.[5, 54]

2. Cluster expansions

The cluster expansion model represents a scalar extensive quantity as a linear expansion in the cluster basis functions of Eq. (5), and was obtained using the ICET software package.[48] The per-site mixing enthalpy for the representative surface alloy was expanded as:

$$\Delta H_{\text{mix}} = \sum_{\alpha} m_{\alpha} J_{\alpha} \bar{\Phi}(\vec{\sigma}_{\alpha}), \quad (16)$$

with the sum taken over all symmetrically distinct clusters up to some maximum size and order, while the coefficients, J_{α} , commonly referred to as the effective cluster interactions (ECIs), describe the strength of a interaction averaged over the lattice. Aside from identity and single site clusters, pairs, triplets, and quadruplet clusters were included in the expansion up to a maximum diameter of 7.0 Å; this large cutoff is used to include the cluster corresponding to the channel shape in Fig. 2B) in the energy expression. This resulted in 34 pair, 280 triplet, and 1445 quadruplet clusters for a total of 1761. The expansion coefficients were trained against DFT fitting data in Fig. 3 using the Automatic

Relevance Determination Regression (ARDR) method implemented in scikit-learn to obtain an optimally sparse set of ECIs and reduce over-fitting yielding 87 non-zero ECIs after training.[55] A weighting function was added based on convex hull distances, by $W = (1 + e^{-\frac{D}{kT}})/(1 - e^{-\frac{D}{kT}})$ where D is the distance between the convex hull and the mixing energy of the configuration, k , Boltzmann's constant, and T the temperature. After optimization of regularization parameters with respect to k=10-fold cross validation, the test error was 8 meV/site. The ECIs as a function of cluster radius and numbers of vertices are given in Fig. 4, with the exception of the identity and single site clusters with ECIs of -14.5 and -1.8 meV, respectively. The relative sizes of the ECIs reflect the relative contribution to the mixing energy for some surface alloy configuration. Relatively large ECIs associated with clusters containing four vertices highlight the importance of interactions beyond pairs in this system.

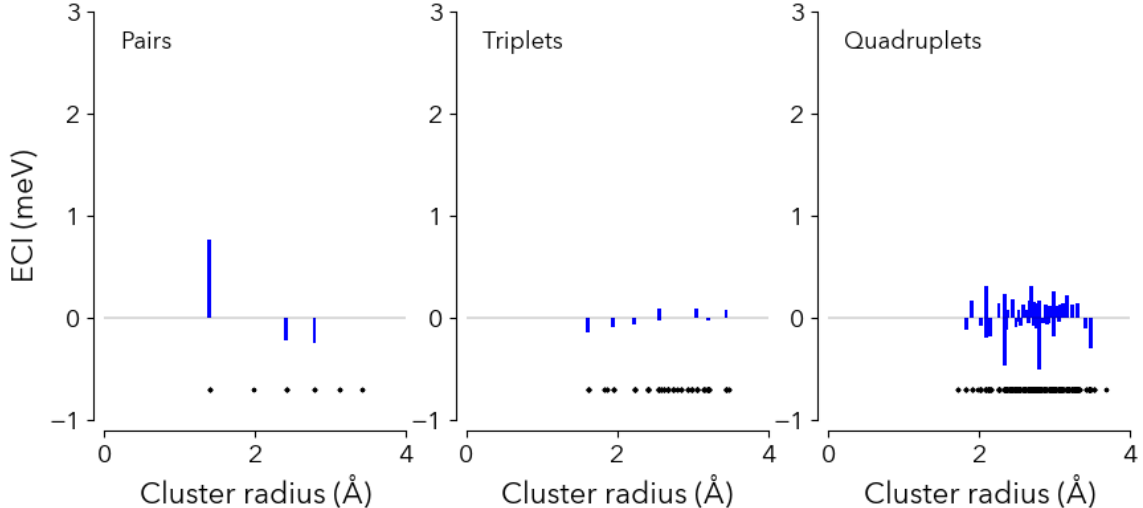


Figure 4: Effective cluster interactions/expansion coefficients for the surface alloy system in contact with the implicit solvent. The blue bars mark the magnitude and sign of the coefficient for pairs, triplet, and quadruplet clusters, order 2, 3, and 4, respectively.

3. Monte Carlo sampling

Using stochastic algorithms, a representative 10×10 (2.7 nm) surface cell was sampled in the canonical ensemble at 473K. Only shells with low concentrations of Pd (1-20% surface content) were considered because of the mechanical destabilization of shells with high palladium content. For each composition, an order parameter was obtained for the chemical ordering motif associated with the the channel shape, a four-point vertically oriented cluster in Fig. 2B along with relevant pair orderings. The relatively accurate predictions of the multi-point orderings were facilitated by sampling converged simulations. The convergence of the parallel Monte Carlo simulations was quantified with the potential scale reduction factor from Brooks and Gelman 1997, which uses the the effective number of independent measurements, $M_{\text{eff}}(k) = 1/[1 + 2\lambda(k)]$, and ratios of pooled and within-simulation variances to quantify the convergence of the parallel chains.[56, 57] Each parallel simulation was ran for 1000 passes after a 100 pass burn-in. The resulting potential scale reduction factors are on the order of 1.00018 and the simulations are considered well converged.[56] The statistical analysis and error measurements are detailed further in the Supporting Information.

The MCHammer Monte Carlo software was used through ICET to carry out Markov-chain Monte Carlo samplings of the surface alloy system.[48, 58] The cluster order parameters were evaluated from the Monte Carlo trajectories using the CLST_ORDER software package developed for this work. The CLST_ORDER python software calculates the normalized, symmetry-averaged probabilities in Eq. (6) for arbitrary cluster shape and order. The parameters can be calculated in general two or three-dimensional crystal systems provided that the atoms can be projected onto pristine parent lattice(s). This software is compatible with the trajectories produced from MCHammer, but can also used with other software packages that generate trajectories or structure files compatible with Atomistic Simulation Environment (ASE) such as the Large-scale Atomic/Molecular Massively Parallel Simulator (LAMMPS) package.[59, 60]

4. Chemical ordering quantification

Chemical ordering analysis for alloys is commonly given in terms of pair ordering in certain nearest neighbor shells. Discussions of multi-point ordering motifs generally involve a consideration of all constituent pair orderings contained in the motif.[24, 34] In the case of the Pd channel, the Pd pair ordering in the 0-3 nearest neighbor shells contained in the channel show some limiting factors for the occurrences of the channels as well as the structure of the alloy overall. Due to the anisotropy of the system along the surface norm, pair orderings in a given neighbor shell are not the same throughout the surface alloy; pairs ordering oriented along the surface norm differs from pair ordering parallel to the surface. For this reason, we extract from the Monte Carlo simulations a set of vertically-oriented pair order parameters that can be used for a Kirkwood superposition of the Pd channel. The order parameters for the Pd-Pd pairs are reported in Fig. 5A) for first nearest neighbors, second nearest neighbors, third nearest neighbors, and average single-site Pd correlations at the bottom and top of the surface alloy (curve with star markers) as a function of Pd fraction. The respective coordination shells are highlighted in the plot. In crystals possessing 3D periodicity, this same model can be applied with averaging pair probabilities over all equivalent orientations and constant single-site correlations that are given simply by the concentrations.

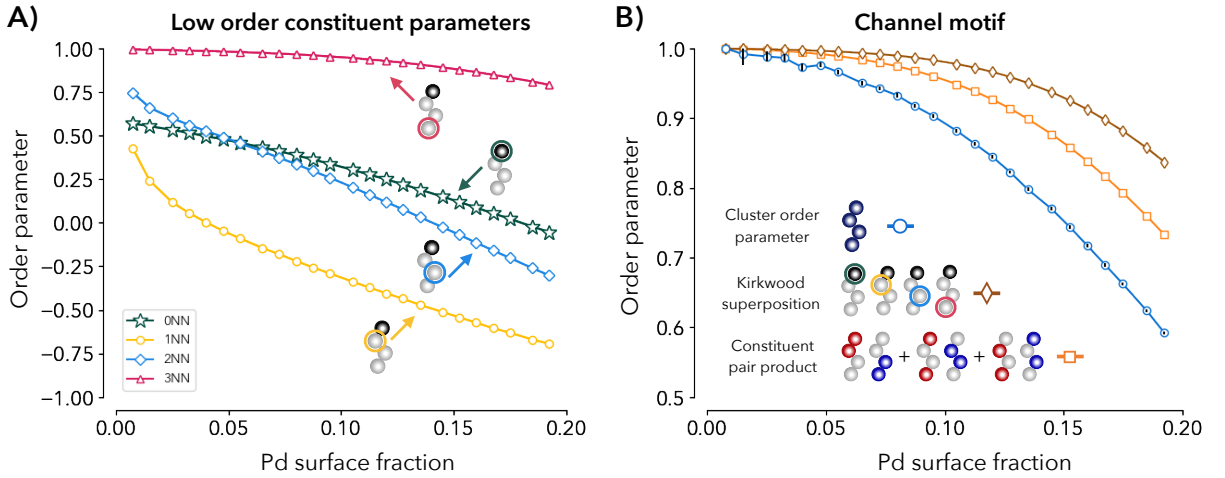


Figure 5: A) The pair parameters for all of the nearest neighbor shells contained in the four-point channel are provided along with the combined single site correlations at the surface and bottom of the alloy. B) The exact four-point order parameter corresponding to the channel-shaped cluster, from direct calculation during MC simulations, with corresponding standard errors (blue circles and black bars), are compared to that calculated from the implementation of the Kirkwood superposition in Clapp 1967 (brown diamonds) as well as the constituent pair products used by Shirley and Wilkins (orange squares).[23, 26, 27] A visualization of low order probabilities used to approximate the four-point channel probability are illustrated for each case.

The parameters in Fig. 5A describe how likely a given Pd-Pd pair is to occur within the channel shape relative to a completely random alloy. Recalling that these parameters are 0 in a completely random alloy, the lower values for the Pd-Pd pairs in the first neighbor shell (circle markers) indicate that Pd-Pd pairs are likely to form at the top or bottom of the surface alloy. The likelihood for the occurrence precursors of the Pd channels is high. In the third shell (triangle markers), the occurrence of Pd-Pd pairs is highly unlikely, and this is one of the key factors that limits the occurrence of Pd channels overall. The Pd tends to reside in the middle of the shell as indicated by the third neighbor shell parameter as well as the single site correlation for the top/bottom of the alloy. This supports the experimental findings of Zhang et al., because a significant amount of Pd remains after etching of the core. This low order analysis that is common in the literature is useful for determining limiting factors for channel occurrence and alloy structure.

Direct quantification the Pd channel occurrences in the surface alloy during the parallel Monte Carlo simulations using the cluster order parameter is reported in Fig. 5B. For the compositions tested the channels occur less frequently than in a randomized alloy lattice, because the results show that the cluster order parameter is greater than 0. The channels occur only in small amounts. This supports the need for small amounts of Pd channels without excess that mechanically destabilizes the shell in experiment. From pair analysis alone one may expect insignificant amounts of Pd channels at experimentally relevant compositions ($\approx 10\%$ Pd) given the limiting formation of third neighbor shell Pd-Pd pairs, Fig. 5A, but there are significant amounts of channels when quantified by the cluster order parameter.

Using the limiting pair parameter alone is not sufficient for quantifying the Pd channel occurrence.

Improved quantification of Pd channels can be made by approximating the four-point probability with combinations of pair probabilities. There are various combination/superposition expressions that could be used to approximate the four-point Pd channel probability, but two key examples are provided for comparison. Using a slightly modified form of Eq. 7 in Ref. [23], the relative four-point probability can be approximated using Kirkwood's superposition,

$$\bar{P}(\vec{\sigma}_\alpha)/P_{\text{random}} \approx P_0 \times P_{01} \times P_{02} \times P_{03}/c_{\text{Pd}}^7, \quad (17)$$

where P_{ij} are the Pd probabilities between the i^{th} and j^{th} neighbor shells and c_{Pd}^7 is product of the marginal probabilities for the constituent pairs and single site correlations. The corresponding approximation to the cluster order parameter is given as the curve with diamond markers in Fig. 5B. This approximation describes some qualitative trends correctly, but deviates from the exact cluster order parameter value. From a consideration of constituent pair probabilities in this way, the amount of Pd channels at low concentrations may still be misleadingly small. One benefit of this approximation is that it can often be obtained from experimentally determined Warren Cowley parameters. Here we point out that the relative standard error for the cluster order parameter ranges between 0.3 % and 99.5 % over the full Pt composition range tested (0.5 - 7.4 % at the experimentally relevant composition range of $c_{\text{Pd}} = 0.05 - 0.15$). The Kirkwood superposition gives a relative standard error range of 0.7 - 1310 % over the full composition range tested (1.2 - 22.8 % at the experimentally relevant composition range of $c_{\text{Pd}} = 0.05 - 0.15$). After propagation of error, the approximation method quantifies the Pd channel occurrence with larger uncertainty than the exact cluster order parameter due to the multiple measurements needed to construct the Kirkwood superposition.

The approximation suggested by Shirley and Wilson in 1977 provides a slightly improved prediction of the exact parameter. For this case, curve with square markers in Fig. 5B, the normalized four-point probability is approximated as,

$$\bar{P}(\vec{\sigma}_\alpha)/P_{\text{random}} \approx (P_{01} \times P_{23} + P_{02} \times P_{13} + P_{03} \times P_{12})/c_{\text{Pd}}^4, \quad (18)$$

While this approximation is somewhat closer to the exact value given by the cluster order parameter, it relies on spatially resolved ordering probabilities that are not obtained from typical experimentally derived pair parameters. As demonstrated in the comparison with the order parameter defined by the exactly calculated cluster probability, these approximations only qualitatively reproduce trends for the Pt/Pd surface alloy.

IV. CONCLUSION

A general cluster order parameter was introduced to systematically quantify multi-point ordering motifs in alloy crystals via direct calculation of cluster probabilities. This parameter can be used to quantify chemical ordering in alloys and substitutional systems that cannot be addressed by pair ordering analysis alone. Though the pair ordering and pair interactions are often most important, there are systems where higher order correlations are significant and cannot be ignored. The utility of the cluster order parameter is that a specific multi-point motif of interest can be quantified directly in simulations or in theoretical applications. In certain special cases where 'clusters' are chosen such that they can represent derivative structures of a crystal, these parameters could be used to help generalize the geometrical locus method.

Despite the expected low probability of occurrence for multi-point ordering motifs, meaningful predictions of cluster order parameters can be made through efficient sampling during parallel Markov-chain Monte Carlo simulations. The average cluster order parameters can be predicted with reasonable certainty with relative standard errors of 0.5 - 7.4 % between the experimentally relevant composition range of $c_{\text{Pd}} = 0.05 - 0.15$. The cluster order parameter quantifies Pd channel occurrence with improved certainty and accuracy over approximate methods such as the Kirkwood superposition. Similar sampling approaches could be used to predict multi-point cluster order parameters in many other practical applications such as descriptors for data-driven materials discovery and machine-learning models of alloy systems.[61] With the multi-lattice generalization, correlations between multiple sublattices can also be described. This generalization is particularly useful for describing ordering between ligand vacancies on one sublattice and alloying metals in another.

The utility of the parameters was demonstrated while modeling representative surfaces of the Pt/Pd nanoparticle alloy system in Fig. 2. Cluster expansion models were generated for a four-layer dilute Pt/Pd alloy on top of a four-layer bulk palladium core region with the (111) surface orientation, and these systems were sampled using Markov-Chain Monte Carlo simulations. In this system, Pd channels that span the surface alloy are needed for the synthesis of high surface area Pt nanocage catalysts. The calculated cluster order parameter corresponding to a channel shape in these simulations suggested that Pd channels occur in significant amounts, enough to occur once or twice in a dilute 10% surface alloy experimental nanoparticle facet sizes, but not with a frequency expected to make the structures

less durable. Using lower order correlations alone to quantify Pd channels leads to a significant underestimation of channel occurrence. Though pair ordering provides a wealth of information about the alloy structure overall and the factors that limit the occurrence of a Pd channel, it provides poor estimates of the true number of channels occurring in the alloy. This is because multi-point energetics are significant in this system. Additional results in the Supporting Information suggest that different solvent environments could aid in the design of nanostructured catalysts that are more durable. Solvation induces a surface enrichment of Pd without completely eliminating the occurrence of Pd channels that span the surface alloy. This was shown by exact quantification of the four-point channel motif where the limiting factors derived from pair ordering alone may lead one to believe that the Pd channels do not occur in significant amounts.

V. DATA AVAILABILITY

The data is available upon reasonable request from the authors. Software to calculate the order parameters is available at https://github.com/jmgoff/clst_order.

VI. ACKNOWLEDGEMENTS

J. M. G., S. B. S., and I. D. acknowledge financial support from the U.S. Department of Energy, Office of Science, Basic Energy Sciences, CPIMS Program, under Award No. DE-SC0018646.

First-principles calculations for this research were performed on the Pennsylvania State University’s ROAR supercomputer.

A portion of the Monte Carlo analysis was performed on the CNMS CADES supercomputer at Oak Ridge National Laboratory

-
- [1] Wolverton, C., Ozoliņš, V. & Zunger, A. First-principles theory of short-range order in size-mismatched metal alloys: Cu-Au, Cu-Ag, and Ni-Au. *Physical Review B* **57**, 4332–4348 (1998). Publisher: American Physical Society.
 - [2] Fisher, J. C. On the strength of solid solution alloys. *Acta Metallurgica* **2**, 9–10 (1954).
 - [3] Zhang, R. *et al.* Short-range order and its impact on the CrCoNi medium-entropy alloy. *Nature* **581**, 283–287 (2020). Number: 7808 Publisher: Nature Publishing Group.
 - [4] Joannopoulos, J. D. & Cohen, M. L. Theory of Short-Range Order and Disorder in Tetrahedrally Bonded Semiconductors. In Ehrenreich, H., Seitz, F. & Turnbull, D. (eds.) *Solid State Physics*, vol. 31, 71–148 (Academic Press, 1976).
 - [5] Han, B. C., VanderVen, A., Ceder, G. & Hwang, B. J. Surface segregation and ordering of alloy surfaces in the presence of adsorbates. *Physical Review B* **72**, 205409 (2005). Publisher: American Physical Society.
 - [6] Zhang, L. *et al.* Platinum-based nanocages with subnanometer-thick walls and well-defined, controllable facets. *Science* **349**, 412–416 (2015). Publisher: American Association for the Advancement of Science Section: Report.
 - [7] Pan, J. *et al.* Perfect short-range ordered alloy with line-compound-like properties in the ZnSnN₂:ZnO system. *npj Computational Materials* **6**, 1–6 (2020). Number: 1 Publisher: Nature Publishing Group.
 - [8] Rost, C. M. *et al.* Entropy-stabilized oxides. *Nature Communications* **6**, 8485 (2015). Number: 1 Publisher: Nature Publishing Group.
 - [9] Cowley, J. M. X-Ray Measurement of Order in Single Crystals of Cu₃Au. *Journal of Applied Physics* **21**, 24–30 (1950). Publisher: American Institute of Physics.
 - [10] Cowley, J. M. An Approximate Theory of Order in Alloys. *Physical Review* **77**, 669–675 (1950). Publisher: American Physical Society.
 - [11] Mirebeau, I., Hennion, M. & Parette, G. First Measurement of Short-Range-Order Inversion as a Function of Concentration in a Transition Alloy. *Physical Review Letters* **53**, 687–690 (1984). Publisher: American Physical Society.
 - [12] Mohri, T., Terakura, K., Takizawa, S. & Sanchez, J. M. First-principles study of short range order and instabilities in AuCu, AuAg and AuPd alloys. *Acta Metallurgica et Materialia* **39**, 493–501 (1991).
 - [13] Schönfeld, B. *et al.* The microstructure of CuAl. *Acta Materialia* **44**, 335–342 (1996).
 - [14] Fernández-Caballero, A., Wróbel, J. S., Mummery, P. M. & Nguyen-Manh, D. Short-Range Order in High Entropy Alloys: Theoretical Formulation and Application to Mo-Nb-Ta-V-W System. *Journal of Phase Equilibria and Diffusion* **38**, 391–403 (2017).
 - [15] Sanchez, J. M., Ducastelle, F. & Gratias, D. Generalized cluster description of multicomponent systems. *Physica A: Statistical Mechanics and its Applications* **128**, 334–350 (1984).
 - [16] Nicholson, D. M. C. *et al.* Relationship between pair and higher-order correlations in solid solutions and other Ising systems. *Journal of Physics: Condensed Matter* **18**, 11585–11594 (2006). Publisher: IOP Publishing.
 - [17] Schweika, W. & Carlsson, A. E. Short-range order in Ising-like models with many-body interactions: Description via effective pair interactions. *Physical Review B* **40**, 4990–4999 (1989). Publisher: American Physical Society.
 - [18] Laks, D. B., Ferreira, L., Froyen, S. & Zunger, A. Efficient cluster expansion for substitutional systems. *Physical Review B* **46**, 12587 (1992).
 - [19] Wolverton, C., Zunger, A. & Schönfeld, B. Invertible and non-invertible alloy Ising problems. *Solid State Communications* **101**, 519–523 (1997).
 - [20] Fontaine, D. D. The number of independent pair-correlation functions in multicomponent systems. *Journal of Applied Crystallography* **4**, 15–19 (1971). eprint: <https://onlinelibrary.wiley.com/doi/pdf/10.1107/S0021889871006174>.
 - [21] Ceguerra, A. V. *et al.* Short-range order in multicomponent materials. *Acta crystallographica. Section A, Foundations of crystallography* **68** (2012).
 - [22] Clapp, P. C. & Moss, S. C. Correlation Functions of Disordered Binary Alloys. I. *Phys. Rev.* **142**, 418–427 (1966).
 - [23] Clapp, P. C. Exact Relations between Triplet Probabilities and Pair Correlations in $\{AB\}$ Binary Alloys and Ising Spin- $\frac{1}{2}$ Systems. *Phys. Rev.* **164**, 1018–1020 (1967).
 - [24] Clapp, P. C. Theoretical determination of n-site configuration probabilities from pair correlations in binary lattices. *Journal of Physics and Chemistry of Solids* **30**, 2589–2598 (1969).
 - [25] Kirkwood, J. G. Statistical Mechanics of Fluid Mixtures. *J. Chem. Phys.* **3**, 300–313 (1935).
 - [26] Shirley, C. G. & Wilkins, S. Many-Site Interactions and Correlations in Disordered Binary Alloys. *Phys. Rev. B* **6**, 1252–1263 (1972).
 - [27] Shirley, C. G. & Wilkins, S. W. Disordered binary alloys. II. Decoupling schemes for many-site correlation functions. *Phys. Rev. B* **16**, 3484–3488 (1977).
 - [28] Clapp, P. C. Atomic Configurations in Binary Alloys. *Phys. Rev. B* **4**, 255–270 (1971).
 - [29] Gratias, D. G. & Cenedese, P. A C.V.M. APPROACH OF MULTIPLET CORRELATION FUNCTIONS IN SUBSTITUTIONAL SOLID SOLUTIONS. *J. Phys. Colloques* **46**, C9–149–C9–153 (1985).
 - [30] De Ridder, R. Iterative method for the calculation of atomic cluster probabilities from pair correlations in binary systems. *Physica A: Statistical Mechanics and its Applications* **79**, 217–232 (1975).
 - [31] Welberry, T. R. & Craig, D. P. Solution of crystal growth disorder models by imposition of symmetry. *Proceedings of the Royal Society of London. A. Mathematical and Physical Sciences* **353**, 363–376 (1977).
 - [32] Welberry, T. Multi-site correlations and the atomic size effect. *Journal of applied crystallography* **19**, 382–389 (1986).
 - [33] Brunel, M., De Bergevin, F. & Gondrand, M. Determination theorique et domaines d existence des differentes surstructures dans les composés a3 b1 x22 de type NaCl. *Journal of Physics and Chemistry of Solids* **33**, 1927–1941 (1972).

- [34] Sauvage, M. & Parthé, E. Prediction of diffuse intensity surfaces in short-range-ordered ternary derivative structures based on sns, nacl, cscl and other structures. *Acta Crystallographica Section A: Crystal Physics, Diffraction, Theoretical and General Crystallography* **30**, 239–246 (1974). Number: 2 Publisher: International Union of Crystallography.
- [35] Dyck, D. v., Conde-Amiano, C. & Amelinckx, S. The diffraction pattern of crystals presenting a digenite type of disorder II. The structure of the digenite-related phases derived by means of the cluster theory. *physica status solidi (a)* **58**, 451–468 (1980). [eprint: https://onlinelibrary.wiley.com/doi/pdf/10.1002/pssa.2210580216](https://onlinelibrary.wiley.com/doi/pdf/10.1002/pssa.2210580216).
- [36] Lehmkuhler, F., Grübel, G. & Gutt, C. Detecting orientational order in model systems by X-ray cross-correlation methods. *Journal of Applied Crystallography* **47**, 1315–1323 (2014). Number: 4 Publisher: International Union of Crystallography.
- [37] Pedrini, B. *et al.* Two-dimensional structure from random multiparticle X-ray scattering images using cross-correlations. *Nature Communications* **4**, 1647 (2013). Number: 1 Publisher: Nature Publishing Group.
- [38] Pedrini, B. *et al.* Model-independent particle species disentanglement by X-ray cross-correlation scattering. *Scientific Reports* **7**, 45618 (2017). Number: 1 Publisher: Nature Publishing Group.
- [39] Lemieux, P.-A. & Durian, D. J. Investigating non-Gaussian scattering processes by using nth -order intensity correlation functions. *J. Opt. Soc. Am. A, JOSAA* **16**, 1651–1664 (1999).
- [40] Zhang, R. *et al.* Direct imaging of short-range order and its impact on deformation in Ti-6Al. *Science Advances* **5**, eaax2799 (2019). Publisher: American Association for the Advancement of Science Section: Research Article.
- [41] Cowley, J. M. Short-Range Order and Long-Range Order Parameters. *Physical Review* **138**, A1384–A1389 (1965). Publisher: American Physical Society.
- [42] Morgan, W. S., Hart, G. L. & Forcade, R. W. Generating derivative superstructures for systems with high configurational freedom. *Computational Materials Science* **136**, 144–149 (2017).
- [43] Tepesch, P. D., Garbulsky, G. D. & Ceder, G. Model for Configurational Thermodynamics in Ionic Systems. *Physical Review Letters* **74**, 2272–2275 (1995). Publisher: American Physical Society.
- [44] Stana, M., Sepiol, B., Kozubski, R. & Leitner, M. Chemical ordering beyond the superstructure in long-range ordered systems. *New Journal of Physics* **18**, 113051 (2016). Publisher: IOP Publishing.
- [45] Mani, P., Srivastava, R. & Strasser, P. Dealloyed pt-cu core-shell nanoparticle electrocatalysts for use in pem fuel cell cathodes. *The Journal of Physical Chemistry C* **112**, 2770–2778 (2008). Publisher: American Chemical Society.
- [46] Alayoglu, S., Nilekar, A. U., Mavrikakis, M. & Eichhorn, B. Ru–Pt core-shell nanoparticles for preferential oxidation of carbon monoxide in hydrogen. *Nature Materials* **7**, 333–338 (2008). Number: 4 Publisher: Nature Publishing Group.
- [47] Stamenkovic, V. R. *et al.* Improved Oxygen Reduction Activity on Pt₃Ni(111) via Increased Surface Site Availability. *Science* **315**, 493–497 (2007). Publisher: American Association for the Advancement of Science Section: Report.
- [48] Ångqvist, M. *et al.* ICET – A Python Library for Constructing and Sampling Alloy Cluster Expansions. *Advanced Theory and Simulations* **2**, 1900015 (2019). [eprint: https://onlinelibrary.wiley.com/doi/pdf/10.1002/adts.201900015](https://onlinelibrary.wiley.com/doi/pdf/10.1002/adts.201900015).
- [49] Andreussi, O., Dabo, I. & Marzari, N. Revised self-consistent continuum solvation in electronic-structure calculations. *The Journal of Chemical Physics* **136**, 064102 (2012). Publisher: American Institute of Physics.
- [50] Giannozzi, P. *et al.* QUANTUM ESPRESSO: a modular and open-source software project for quantum simulations of materials. *Journal of Physics: Condensed Matter* **21**, 395502 (2009). Publisher: IOP Publishing.
- [51] van Setten, M. J. *et al.* The PseudoDojo: Training and grading a 85 element optimized norm-conserving pseudopotential table. *Computer Physics Communications* **226**, 39–54 (2018).
- [52] Marzari, N., Vanderbilt, D., DeVita, A. & Payne, M. C. Thermal Contraction and Disorder of the Al(110) Surface. *Physical Review Letters* **82**, 3296–3299 (1999). Publisher: American Physical Society.
- [53] Huang, J. *et al.* Potential-induced nanoclustering of metallic catalysts during electrochemical CO₂ reduction. *Nature Communications* **9**, 3117 (2018). Number: 1 Publisher: Nature Publishing Group.
- [54] Cao, L., Niu, L. & Mueller, T. Computationally generated maps of surface structures and catalytic activities for alloy phase diagrams. *Proceedings of the National Academy of Sciences* **116**, 22044–22051 (2019). Publisher: National Academy of Sciences Section: PNAS Plus.
- [55] Pedregosa, F. *et al.* Scikit-learn: Machine Learning in Python. *MACHINE LEARNING IN PYTHON* **6**.
- [56] Brooks, S. P. & Gelman, A. General Methods for Monitoring Convergence of Iterative Simulations. *Journal of Computational and Graphical Statistics* **7**, 434–455 (1998). Publisher: Taylor & Francis.
- [57] Gelman, A. & Rubin, D. B. Inference from Iterative Simulation Using Multiple Sequences. *Statistical Science* **7**, 457–472 (1992). Publisher: Institute of Mathematical Statistics.
- [58] Foreman-Mackey, D., Hogg, D. W., Lang, D. & Goodman, J. emcee: The MCMC Hammer. *Publications of the Astronomical Society of the Pacific* **125**, 306–312 (2013). Publisher: IOP Publishing.
- [59] Larsen, A. H. *et al.* The atomic simulation environment—a Python library for working with atoms. *Journal of Physics: Condensed Matter* **29**, 273002 (2017). Publisher: IOP Publishing.
- [60] Plimpton, S. Fast Parallel Algorithms for Short-Range Molecular Dynamics. *Journal of Computational Physics* **117**, 1–19 (1995).
- [61] Jennings, P. C., Lysgaard, S., Hummelshøj, J. S., Vegge, T. & Bligaard, T. Genetic algorithms for computational materials discovery accelerated by machine learning. *npj Computational Materials* **5**, 1–6 (2019). Number: 1 Publisher: Nature Publishing Group.